COMMENTS AND OPINIONS

Journal of Semiconductors
(2021) 42, 050301
doi: 10.1088/1674-4926/42/5/050301

Over 1 cm^2 flexible organic solar cells

Wei Pan[1], Yunfei Han[1], Zhenguo Wang[1], Qun Luo[1, †], Changqi Ma[1, †], and Liming Ding[2, †]

[1]Pintable Electronics Research Center, Suzhou Institute of Nano-Tech and Nano-Bionics (CAS), Suzhou 215123, China

[2]Center for Excellence in Nanoscience (CAS), Key Laboratory of Nanosystem and Hierarchical Fabrication (CAS), National Center for Nanoscience and Technology, Beijing 100190, China

Citation: W Pan, Y F Han, Z G Wang, Q Luo, C Q Ma, and L M Ding, Over 1 cm^2 flexible organic solar cells[J]. *J. Semicond.*, 2021, 42(5), 050301. http://doi.org/10.1088/1674-4926/42/5/050301

Organic solar cells (OSCs) have received considerable attention and demonstrated great potential as flexible, lightweight, semitransparent, and low-cost energy sources. Flexible OSCs have practical applications in wearable electronics, portable chargers for back bags and tents, solar airships, *etc.* Many efforts have been made to improve the performance of flexible OSCs, including the development of flexible transparent electrodes, new organic materials, and optimization of the device structure. Progresses have been achieved in the last few years, and power conversion efficiencies (PCEs) of 16.1%[1], 16.5%[2], 13.61%[3], and 10.09%[4] for 0.04 cm^2 single-junction device, 0.04 cm^2 tandem device, 1 cm^2 single-junction device, and 25 cm^2 module were reported.

Flexible transparent electrodes are the essential components for flexible OSCs, which should possess high electrical conductivity, transparency, and excellent mechanical flexibility. Flexible ITO is the most widely used transparent electrode. Because of the brittleness, high sheet resistance and high cost of flexible ITO electrodes[5], cost-effective and flexible transparent electrodes are still highly needed. Various ITO-free electrodes, such as metal mesh, metal nanowires, graphene, carbon nanotube, were developed and applied in flexible OSCs. Fig. 1 shows the comparison of the conductivity and light transparency of various transparent electrodes. The metal electrodes, including the thin metal, metal grid, and metal nanowire have good conductivity. However, the thin metal can give a relative low transmittance around 40%–60%. The carbon-involved transparent electrode, *i.e.* CNT and graphene, and PEDOT:PSS electrode have good optical transmittance around 70%–80%. However, they show relative lower electrical conductivity with sheet resistance as high as 100 Ω/□. Overall, among these electrodes, metal grid and Ag nanowires are among the best choices due to their good average visible transmittance (AVT 80%) and relatively low sheet resistance (R_s ~10 Ω/□) [6].

The metal mesh electrodes were made by thermal evaporation[7], flexo printing[8], or inkjet printing[7, 9]. These mesh electrodes have lower sheet resistance of several Ω/□. However, the light transmittance was relatively low (< 80%) because the grid width are usually larger than 10 μm. In contrast, the metal mesh electrodes made by nanoimprinting method have advantages both in conductivity and transparency. The line width of the metal mesh can be reduced to < 3 μm, which is invisible to the naked eyes and ensures a good transparency. This electrode showed an average transmittance > 85%. Since a thick Ag layer (~ 3 μm) was embedded in the substrate, the electrode has excellent conduction with sheet resistance < 5 Ω/□. The performance of OSCs is highly sensitive to the conductivity of the transparent electrode, especially when the cell area is > 1 cm^2[10], so this type of electrode is quite suitable for large-area flexible solar cells. Chen *et al.* first reported the use of metal grid electrodes in flexible OSCs[11], and an efficiency of 5.85% was achieved for a 1.21 cm^2 OSC[10]. Following this, Tan[12] and Wu *et al.*[13] reported OSCs with these electrodes. To smooth the surface of the silver nanogrid and to increase the conductivity of the final electrode, Su *et al.* developed new silver nanogrid/copper (Ag-NG/Cu) or silver nanogrid/Ni composite electrode by applying Cu or Ni electroplating and the following surface polishing steps[14], and a lowest sheet resistance of 0.03 Ω/□ was obtained. The highest figure of merit (FOM) reached 8 × 10^4[15]. Ma *et al.* reported the flexible OSCs with Ag-NG/Cu electrode. By modifying electrode surface, power conversion efficiencies (PCEs) of 8.75%, 7.79% and 7.35% for 2.4, 4.0, and 9.0 cm^2 cells were achieved, respectively, which are higher than that of devices with flexible ITO electrode (6.61% and 5.88% for 2.4 and 4.0 cm^2 cells, respectively) (Fig. 2)[16]. The Ag/Cu composite grid-involved flexible cells could maintain 91.7%, 81.7%, and 77.0% efficiency of the 1 cm^2 cell as the area increased to 2.4, 4.0, and 9.0 cm^2, respectively, while the efficiency for flexible ITO device decreased to 74.6% (for 2.4 cm^2) and 66.4% (for 4 cm^2) of the 1 cm^2 cells, clearly demonstrating that lowering the sheet resistance of the transparent electrode is helpful in achieving high performance for large-area solar cells.

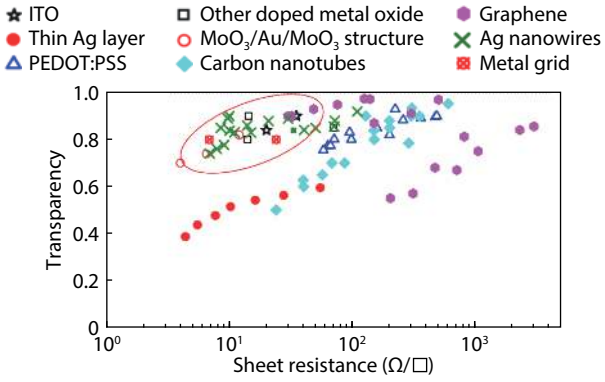

Fig. 1. (Color online) Transparency and sheet resistance of the transparent conducting electrodes (reproduced with copyright permission from SPIE publisher)[6].

Correspondence to: Q Luo, qluo2011@sinano.ac.cn; C Q Ma, cqma2011@sinano.ac.cn; L M Ding, ding@nanoctr.cn

Received 6 FEBRUARY 2021.

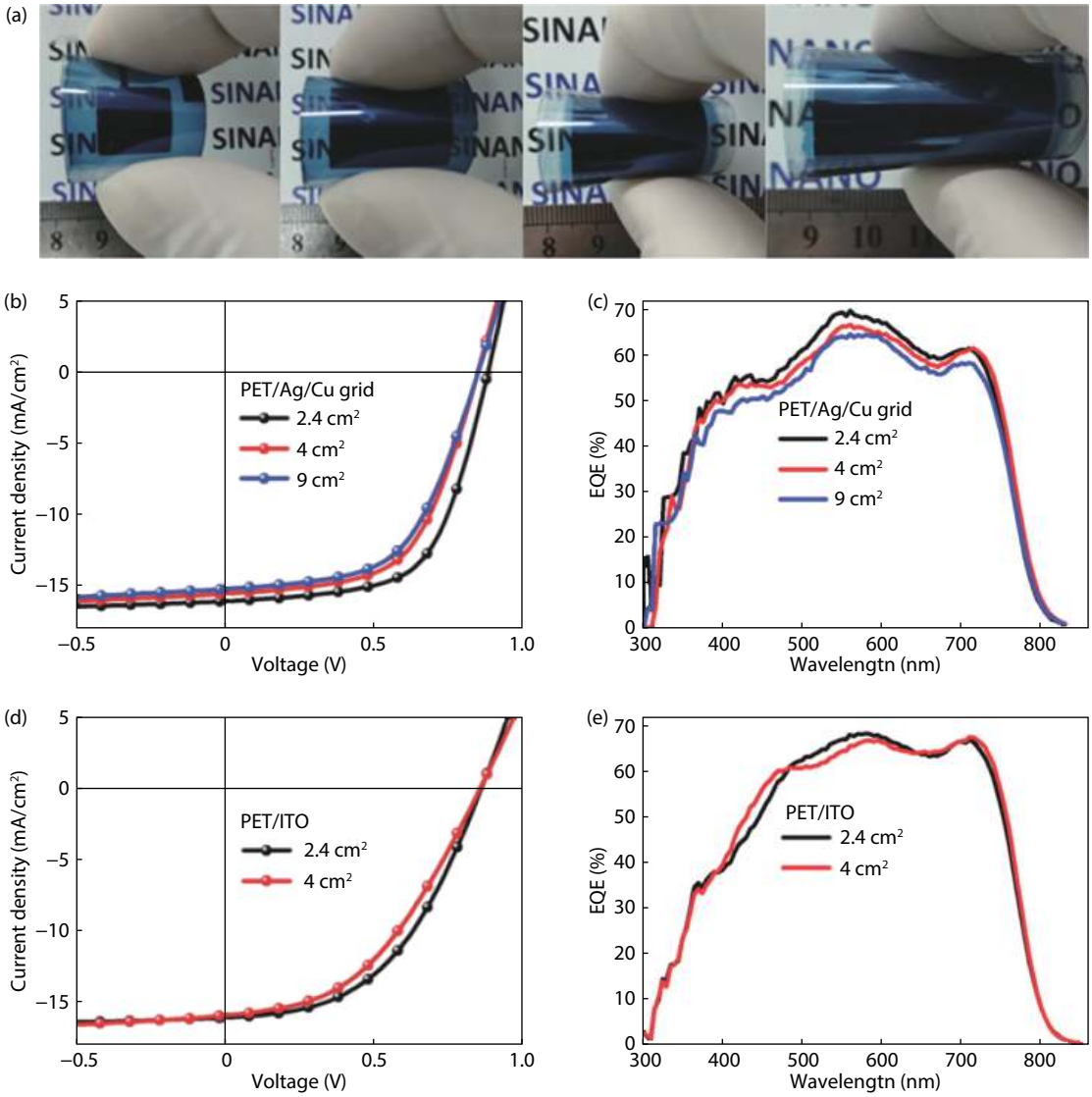

Fig. 2. (Color online) (a) Photographs of the large-area flexible OSCs. (b) *J*–*V* characteristics and (c) EQE spectra of the large-area flexible solar cells with PET/Ag/Cu grid electrodes. (d) *J*–*V* characteristics and (e) EQE spectra of the large-area flexible solar cells with PET/ITO electrodes (reproduced with copyright permission from Wiley-VCH)[16].

Very recently, Wei *et al.* reported flexible OSC module with Ag-NG electrode *via* slot-die coating (Fig. 3). Owing to the difference in film formation kinetics between spin-coating and slot-die coating, controlling of the film morphology is critical for large-area fabrication. By applying hot substrates and non-halogen solvent, a PCE of > 10% was achieved for the printed cell with an area of 25 cm^2, which is the highest PCE for a flexible cell with > 10 cm^2 area.

In addition to silver nanogrid electrode, nanowires (AgNW) networks are also good candidates for the preparation of large-area flexible solar cells due to their balanced light transparency and conductivity. Both AgNW and AgNW composite electrodes[17] were prepared through various solution-processed methods, including spin-coating[18, 19], slot-die coating[20], brush printing[21]. The sheet resistances of AgNW electrode are generally 10–20 Ω/□, and transmittance can be as high as 85%–92%. The conductivity of AgNW electrode is determined by the connection of Ag nanowires. The removal of polyvinylpyrrolidone (PVP) surfactant and the welding of the nanowire can improve the conductivity[22]. Choy *et al.* developed an one-step multifunctional chemical treatment for AgNW/PEDOT:PSS composite electrode[23].

ITO is widely used in optoelectronic devices. The flexible ITO electrode is not good at mechanical and conductive properties. Though the sheet resistance of ITO can reach to 10 Ω/□, the flexible ITO has higher sheet resistance (40–60 Ω/□). The use of flexible ITO electrode in OSCs with area > 1 cm^2 was rarely reported, especially in recent years. Tables 1 and 2 show the development of flexible OSCs (> 1 cm^2 single cells and the flexible modules). A PCE of 5.25% for 80 cm^2 flexible OSC modules with flexible ITO electrode was reported[24].

Spin-coating, slot-die coating and brush printing are not pre-patternable, and a laser scribing process is needed for making a structured electrode. Very recently, Ma *et al.*[3] reported the preparation of large-area patterned AgNW electrode through a gravure printing process. Fig. 4(a) shows the schematic diagram of gravure printing process. The printing process contains three steps: (1) the doctor blade forces the ink to fill the gravure cavities; (2) the ink is transferred from the cavities of the gravure roller to the substrate; (3) ink leveling on the substrate. The AgNW electrode can be easily patterned by using a pre-patterned gravure roller. In addition,

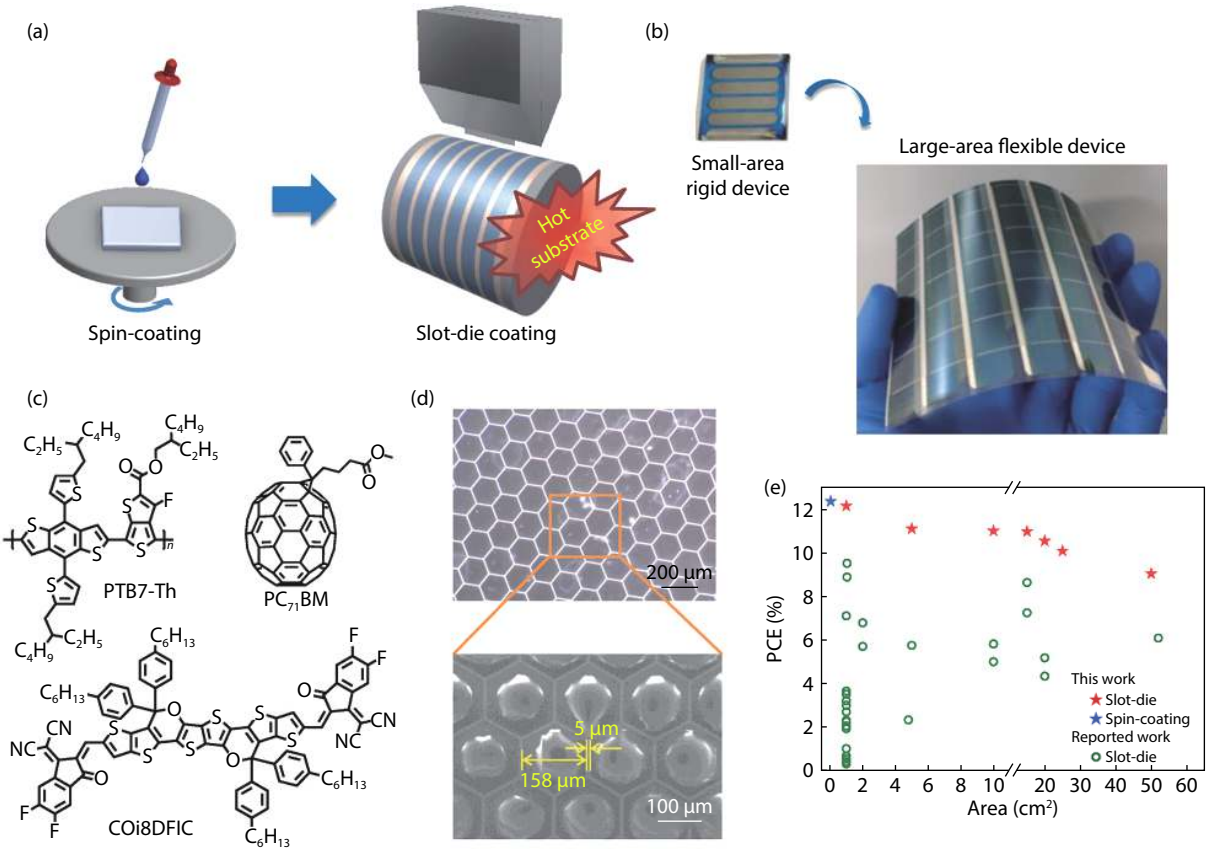

Fig. 3. (Color online) (a) Sketch of spin coating and slot-die coating. (b) The small-area rigid device and large-area flexible device. (c) The chemical structures of PTB7-Th, $PC_{71}BM$, and COi8DFIC. (d) Optical microscopy and SEM images of the PET/silver-grid substrate. (e) Comparison of this work with reported PCEs for flexible devices made by slot-die coating (reproduced with copyright permission from Wiley-VCH)[4].

Table 1. The performance data for large-area flexible OSCs (> 1 cm^2) (Fig. 5).

Year	Area (cm^2)	PCE (%)	Electrode	Device structure	Fabrication technique	Ref.
2005	1.2	1	PEDOT:PSS	PEDOT:PSS/α-NPD/C_{60}/BCP/Mg:Al	Spin coating	[36]
2007	10	1.6	ITO	PET/ITO/PEDOT:PSS/P3HT:PCBM/Al	Doctor blading	[37]
2009	1	2.7	ITO	PET/ITO/ZnO/P3HT:PCBM/PEDOT:PSS/Silver	Screen printing	[38]
2010	4	1.93	Ag grid	PEN/Ag grid/HC-PEDOT/P3HT:PCBM/LiF/Al	Spin coating	[39]
2013	1.21	1.36	Ag grid	PET/Ag grid/PH1000/PEDOT:PSS-4083/P3HT:PCBB-C8/LiF/Al	Spin coating	[11]
2014	1.21	5.85	Ag grid	PET/Ag grid/PH1000/ZnO/PFN/PTB7:$PC_{71}BM$/MoO_3/Ag	Spin coating	[10]
2015	4	7.09	Ag	PET/Ag/PFN/PTB7-Th:$PC_{71}BM$/MoO_3/Ag/MoO_3	Spin coating	[34]
2017	1.25	8.28	Ag grid	PET/Ag grid/PTB7-Th:p-DTS(FBTTH$_2$)$_2$:$PC_{71}BM$/MoO_3/Ag	Slot-die	[40]
2018	2.03	7.6	Ag/TiO_x	Ag/TiO_x/ZnO/PTB7-Th:ITIC/PEDOT:PSS	Doctor blading	[41]
2019	1	12.26	Ag/Cu grid	PET/Ag/Cu grid/E100/ZnO/PBDB-TF:IT-4F/MoO_3/Al	Spin coating	[16]
2020	1	13.6	Ag NWs	PET/Ag NWs/ZnO/PM6:Y6/MoO_3/Al	Spin coating	[3]

Table 2. The performance data for flexible OSC modules (Fig. 5).

Year	Area (cm^2)	PCE (%)	Electrode	Device structure	Fabrication technique	Ref.
2005	16.8	0.04	PEDOT:PSS	PET/PEDOT:PSS/MDMO-PPV:PCBM/Al	Doctor blading	[42]
2007	17.1	1.5	ITO	PET/ITO/PEDOT:PSS/P3HT:PCBM/Al	Doctor blading	[37]
2008	53	2.52	ITO	PET/ITO/ PEDOT:PSS/P3HT:PCBM/ LiF/Al	Spin coating	[43]
2009	120	2.1	ITO	PET/ITO/ZnO/P3HT:PCBM/PEDOT:PSS/Silver	Screen printing	[38]
2013	66	1.6	Ag grid	PET/Ag grid/PEDOT:PSS/ZnO/P3HT:PCBM/PEDOT:PSS/Ag grid	Slot-die	[44]
2014	8	3	Ag grid	PET/Ag grid/PEDOT/ZnO/PDTSTTz-4:PCBM/PEDOT/Ag	Slot-die	[45]
2016	35	4.2	FTO	PET/FTO/PBTZT-stat-BDTT-8:PCBM/PEDOT:PSS/Ag	Slot-die	[46]
2017	10.5	6.5	Ag	PES/Ag/PEI/P3HT:ICBA/PEI:m-PEDOT:PSS/PTB7-Th:PCBM/PEDOT:PSS/Ag grid	Spin coating	[47]
2019	15	8.9	ITO	PET/ITO/ZnO/active layer (PTB7-Th: PC71BM or PBDB-T: ITIC)/MoO_3/Ag	Slot-die	[27]
2020	25	10.09	Ag grid	PET/Ag grid/ZnO/PTB7-Th:COi8DFIC:PC71BM/MoO_3/Ag	Slot-die	[4]

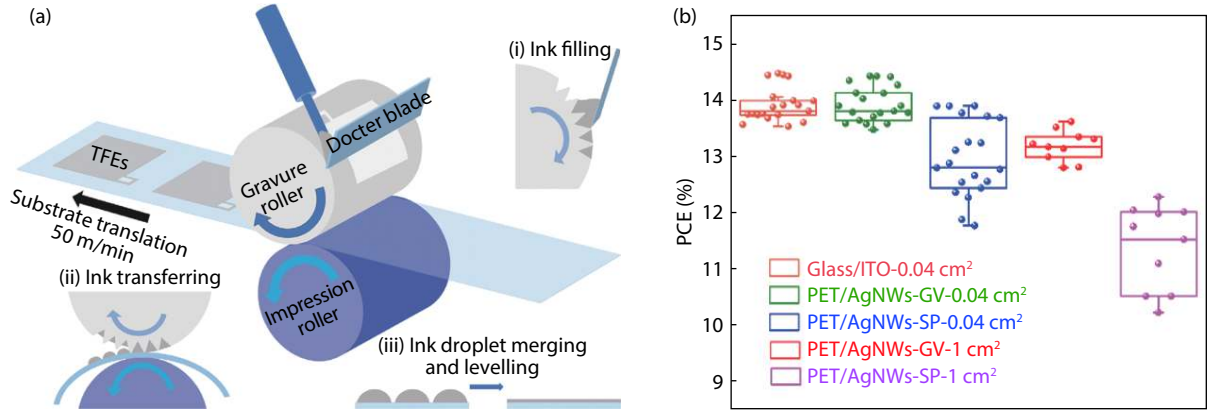

Fig. 4. (Color online) (a) Schematic diagram for the high-speed gravure printing process used to print silver nanowire electrodes. (b) Efficiency distribution diagram for the devices with PET/AgNWs-GV, PET/AgNWs-SP, and glass/ITO electrodes (reproduced with copyright permission from Wiley-VCH)[3].

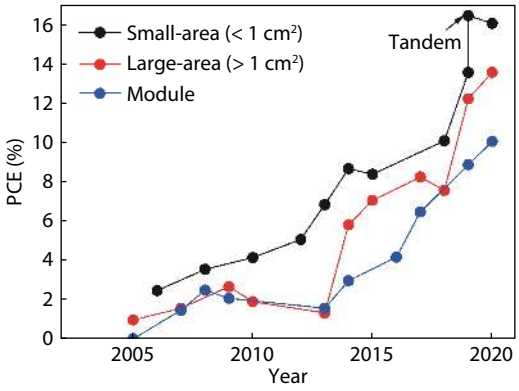

Fig. 5. (Color online) The PCEs for small-area OSCs[1, 2, 28–35], large-area OSCs (>1 cm²)[3, 10, 11, 16, 36–41], and flexible OSC modules[4, 27, 37, 38, 42–47].

gravure printing is extremely suitable for large-scale fabrication because of its high printing speed. To meet the requirement of gravure printing, the ink needs to be optimized to have suitable surface tension, volatilization rate, and viscosity. After careful ink formulation and printing process optimization, the gravure-printed AgNW electrode showed a high light transmittance of 95.4% (excluding PET substrate) and low sheet resistance of ~ 10 Ω/□ with excellent homogeneity. An efficiency of 13.61% (certified 12.88%) was achieved for 1 cm² cells with printed AgNW electrode (Fig. 4(b)). Interestingly, the cells with gravure-printed AgNW electrode (AgNW-GV) presented much narrower PCE distribution than the cells with spin-coated AgNW electrode (AgNW-SP), which might be due to the homogenously distributed cavities.

Since the first report on flexible OSCs in 2004, the efficiency for small-area flexible OSCs (< 1 cm²) has increased from ~1% to 16.5%. The efficiency of middle-sized cells (≥ 1 cm²) is lower than that of the small cells (Fig. 5), due to the unavoidable increase of series resistance of the electrode. Interestingly, PCEs of both small and middle-sized flexible OSCs increase fast after 2016, which is due to the development of high-performance non-fullerene acceptors IT-4F[25] and Y6[26], and also the development of high-performance flexible metal-nanogrid and nanowire electrodes. From Tables 1 and 2, the large-area flexible single OSCs and the flexible OSC modules usually used Ag nanowire and Ag grid as the flexible electrodes, demonstrating the great potential of these flexible electrodes in upscaling flexible OSCs. Higher PCE is expected to be achieved in next few years with the fast development of transparent electrodes and new methods for preparing flexible solar modules[24, 27].

Many advances have been made in flexible OSCs in the last few years, and > 10% PCE was realized for the flexible solar modules, moving one big step toward the real application of flexible OSCs. However, there exist two critical issues: scaling-up and encapsulation. As the layer thickness and nanomorphology of the photoactive layer might be different at different sites (e.g. the edge *vs* the center), a good way to control the drying process of the printed organic thin films is very important. Sequential deposition technology[48], temperature control on solution and substrate[49], *etc* were applied in slot-die coating and blade coating. For the upscaling, the homogeneity controlling is another challenge. The homogeneity is not only affected by the drying process, but also by the interface contact[50]. Thus, the electrode, the quality of the interface layer and the active layer should be well controlled. Gravure printing could be a promising method for making homogeneous large-area OSCs. Very recently, Kim *et al.*[51] reported the preparation of flexible perovskite solar cells, indicating the potential of gravure printing. As for thin film encapsulation, experiences from OLED industry could be helpful, where iterative organic/inorganic thin films showed excellent blocking function to water vapor and oxygen. Thin polymer layers ensure a good flexibility for the encapsulation film, while the condense inorganic layer act as barrier against water vapor and oxygen. Applying all these strategies well, we expect that flexible OSC modules will be in the market soon.

Acknowledgements

We thank National Natural Science Foundation of China (51773224), the Youth Association for Promoting Innovation (CAS) (2019317), and the Strategic Priority Research Program of Chinese Academy of Sciences (XDA09020201) for financial support. L. Ding thanks the National Key Research and Development Program of China (2017YFA0206600) and the National Natural Science Foundation of China (51773045, 21772030, 51922032, 21961160720) for financial support.

References

[1] Qu T Y, Zuo L J, Chen J D, et al. Biomimetic electrodes for flexible

organic solar cells with efficiencies over 16%. Adv Opt Mater, 2020, 8, 2000669
[2] Sun Y N, Chang M J, Meng L X, et al. Flexible organic photovoltaics based on water-processed silver nanowire electrodes. Nat Electron, 2019, 2, 513
[3] Wang Z, Han Y, Yan L, et al. High power conversion efficiency of 13.61% for 1 cm^2 flexible polymer solar cells based on patternable and mass-producible gravure-printed silver nanowire electrodes. Adv Funct Mater, 2020, 2007276
[4] Wang G D, Zhang J Q, Yang C, et al. Synergistic optimization enables large-area flexible organic solar cells to maintain over 98% PCE of the small-area rigid devices. Adv Mater, 2020, 32, 2005153
[5] Chen Z, Cotterell B, Wang W. The fracture of brittle thin films on compliant substrates in flexible displays. Eng Fract Mech, 2002, 69, 597
[6] Cao W R, Li J, Chen H Z, et al. Transparent electrodes for organic photoelectronic devices: A review. J Photonics Energy, 2014, 4, 040990
[7] Galagan Y, Zimmermann B, Coenen E W C, et al. Current collecting grids for ITO-free solar cells. Adv Energy Mater, 2012, 2, 103
[8] Andersen T R, Dam H F, Hosel M, et al. Scalable, ambient atmosphere roll-to-roll manufacture of encapsulated large area, flexible organic tandem solar cell modules. Energy Environ Sci, 2014, 7, 2925
[9] Galagan Y, Coenen E W C, Sabik S, et al. Evaluation of ink-jet printed current collecting grids and busbars for ITO-free organic solar cells. Sol Energy Mater Sol Cells, 2012, 104, 32
[10] Mao L, Chen Q, Li Y W, et al. Flexible silver grid/PEDOT:PSS hybrid electrodes for large area inverted polymer solar cells. Nano Energy, 2014, 10, 259
[11] Li Y W, Mao L, Gao Y L, et al. ITO-free photovoltaic cell utilizing a high-resolution silver grid current collecting layer. Sol Energy Mater Sol Cells, 2013, 113, 85
[12] Tan L C, Wang Y L, Zhang J W, et al. Highly efficient flexible polymer solar cells with robust mechanical stability. Adv Sci, 2019, 6, 1801180
[13] Wu Q, Guo J, Sun R, et al. Slot-die printed non-fullerene organic solar cells with the highest efficiency of 12.9% for low-cost pv-driven water splitting. Nano Energy, 2019, 61, 559
[14] Chen X L, Guo W R, Xie L M, et al. Embedded Ag/Ni metal-mesh with low surface roughness as transparent conductive electrode for optoelectronic applications. ACS Appl Mater Interfaces, 2017, 9, 37048
[15] Chen X L, Nie S H, Guo W R, et al. Printable high-aspect ratio and high-resolution Cu grid flexible transparent conductive film with figure of merit over 80000. Adv Electron Mater, 2019, 5, 1800991
[16] Han Y, Chen X, Wei J, et al. Efficiency above 12% for 1 cm^2 flexible organic solar cells with Ag/Cu grid transparent conducting electrode. Adv Sci, 2019, 6, 1901490
[17] Tang H H, Feng H R, Wang H K, et al. Highly conducting mxene-silver nanowire transparent electrodes for flexible organic solar cells. ACS Appl Mater Interfaces, 2019, 11, 25330
[18] Chen X B, Xu G Y, Zeng G, et al. Realizing ultrahigh mechanical flexibility and > 15% efficiency of flexible organic solar cells via a "welding" flexible transparent electrode. Adv Mater, 2020, 32, 198478
[19] Dong X Y, Shi P, Sun L L, et al. Flexible nonfullerene organic solar cells based on embedded silver nanowires with an efficiency up to 11.6%. J Mater Chem A, 2019, 7, 1989
[20] Zhang Y X, Fang J, Li W, et al. Synergetic transparent electrode architecture for efficient non-fullerene flexible organic solar cells with >12% efficiency. ACS Nano, 2019, 13, 4686
[21] Kang S B, Noh Y J, Na S I, et al. Brush-painted flexible organic solar cells using highly transparent and flexible Ag nanowire network electrodes. Sol Energy Mater Sol Cells, 2014, 122, 152
[22] Lu H F, Ren X G, Ouyang D, et al. Emerging novel metal electrodes for photovoltaic applications. Small, 2018, 14, 1703140
[23] Kim J, Ouyang D, Lu H F, et al. High performance flexible transparent electrode via one-step multifunctional treatment for Ag nanonetwork composites semi-embedded in low-temperature-processed substrate for highly performed organic photovoltaics. Adv Energy Mater, 2020, 10, 1903919
[24] Han Y W, Jeon S J, Lee H S, et al. Evaporation-free nonfullerene flexible organic solar cell modules manufactured by an all-solution process. Adv Energy Mater, 2019, 9, 1902065
[25] Zhao W C, Li S S, Yao H F, et al. Molecular optimization enables over 13% efficiency in organic solar cells. J Am Chem Soc, 2017, 139, 7148
[26] Yuan J, Zhang Y Q, Zhou L Y, et al. Single-junction organic solar cell with over 15% efficiency using fused-ring acceptor with electron-deficient core. Joule, 2019, 3, 1140
[27] Meng X, Zhang L, Xie Y, et al. A general approach for lab-to-manufacturing translation on flexible organic solar cells. Adv Mater, 2019, 31, 1903649
[28] Huang J, Wang X, Kim Y, et al. High efficiency flexible ITO-free polymer/fullerene photodiodes. Phys Chem Chem Phys, 2006, 8, 3904
[29] Hau S K, Yip H L, Baek N S, et al. Air-stable inverted flexible polymer solar cells using zinc oxide nanoparticles as an electron selective layer. Appl Phys Lett, 2008, 92, 253301
[30] Wang J C, Weng W T, Tsai M Y, et al. Highly efficient flexible inverted organic solar cells using atomic layer deposited ZnO as electron selective layer. J Mater Chem, 2010, 20, 862
[31] Stec H M, Hatton R A. Plasmon-active nano-aperture window electrodes for organic photovoltaics. Adv Energy Mater, 2013, 3, 193
[32] Jose da Silva W, Kim H P, Rashid bin Mohd Yusoff A, et al. Transparent flexible organic solar cells with 6.87% efficiency manufactured by an all-solution process. Nanoscale, 2013, 5, 9324
[33] Zhao B, He Z, Cheng X, et al. Flexible polymer solar cells with power conversion efficiency of 8.7%. J Mater Chem C, 2014, 2, 5077
[34] Zuo L, Zhang S, Li H, et al. Toward highly efficient large-area ITO-free organic solar cells with a conductance-gradient transparent electrode. Adv Mater, 2015, 27, 6983
[35] Song W, Fan X, Xu B, et al. All-solution-processed metal-oxide-free flexible organic solar cells with over 10% efficiency. Adv Mater, 2018, 30, 1800075
[36] Kushto G P, Kim W, Kafafi Z H. Flexible organic photovoltaics using conducting polymer electrodes. Appl Phys Lett, 2005, 86, 093502
[37] Lungenschmied C, Dennler G, Neugebauer H, et al. Flexible, long-lived, large-area, organic solar cells. Sol Energy Mater Sol Cells, 2007, 91, 379
[38] Krebs F C, Gevorgyan S A, Alstrup J. A roll-to-roll process to flexible polymer solar cells: Model studies, manufacture and operational stability studies. J Mater Chem, 2009, 19, 5442
[39] Galagan Y, Rubingh J E, Andriessen R, et al. ITO-free flexible organic solar cells with printed current collecting grids. Sol Energy Mater Sol Cells, 2011, 95, 1339
[40] Zhang J, Zhao Y, Fang J, et al. Enhancing performance of large-area organic solar cells with thick film via ternary strategy. Small, 2017, 13, 1700388
[41] Lin Y, Jin Y, Dong S, et al. Printed nonfullerene organic solar cells with the highest efficiency of 9.5%. Adv Energy Mater, 2018, 8, 1701942
[42] Dennler G, Lungenschmied C, Neugebauer H, et al. Flexible, conjugated polymer-fullerene-based bulk-heterojunction solar cells: basics, encapsulation, and integration. J Mater Res, 2005, 20, 3224
[43] Tsakalakos L, Lemaitre N, de Bettignies R, et al. High-efficiency large area flexible organic solar cells. 2008, 7047, 70470K
[44] Hösel M, Søndergaard R R, Jørgensen M, et al. Fast inline roll-to-roll printing for indium-tin-oxide-free polymer solar cells using

automatic registration. Energy Technol, 2013, 1, 102
[45] Carlé J E, Helgesen M, Madsen M V, et al. Upscaling from single cells to modules – fabrication of vacuum- and ITO-free polymer solar cells on flexible substrates with long lifetime. J Mater Chem C, 2014, 2, 1290
[46] Lucera L, Machui F, Kubis P, et al. Highly efficient, large area, roll coated flexible and rigid opv modules with geometric fill factors up to 98.5% processed with commercially available materials. Energy Environ Sci, 2016, 9, 89
[47] Mao L, Tong J H, Xiong S X, et al. Flexible large-area organic tandem solar cells with high defect tolerance and device yield. J Mater Chem A, 2017, 5, 3186
[48] Dong S, Zhang K, Xie B M, et al. High-performance large-area organic solar cells enabled by sequential bilayer processing via non-halogenated solvents. Adv Energy Mater, 2019, 9, 1802832
[49] Zhao H, Naveed H B, Lin B J, et al. Hot hydrocarbon-solvent slot-die coating enables high-efficiency organic solar cells with temperature-dependent aggregation behavior. Adv Mater, 2020, 32, 2002302
[50] Ji G Q, Zhao W C, Wei J F, et al. 12.88% efficiency in doctor-blade coated organic solar cells through optimizing the surface morphology of a ZnO cathode buffer layer. J Mater Chem A, 2019, 7, 212
[51] Kim Y Y, Yang T Y, Suhonen R, et al. Gravure-printed flexible perovskite solar cells: Toward roll-to-roll manufacturing. Adv Sci, 2019, 6, 1802094

Wei Pan is a MS student in Suzhou Institute of Nano-Tech and Nano-Bionics (CAS). He obtained his BS from Wuhan Institute of Technology in 2018. His work focuses on interface engineering in flexible/large-area organic solar cells.

Qun Luo received her PhD form Zhejiang University in 2011. Then she worked as a postdoc at Suzhou Institute of Nano-Tech and Nano-Bionics (CAS). Currently she is an associate professor at Suzhou Institute of Nano-Tech and Nano-Bionics. Her research interests include inks for printed photovoltaics and interface engineering in flexible/large-area printed solar cells.

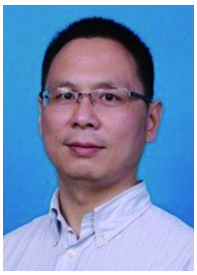

Changqi Ma received his PhD at the Technical Institute of Physics and Chemistry (CAS) with Professor Baowen Zhang. After that, he worked as a postdoc at Heriot-Watt University (UK) with Dr. Graeme Cooke, and then he joined Peter Bäuerle group at University of Ulm in 2004 as a Humboldt fellow. From January 2007 to May 2011, he did his Habilitation at Institute of Organic Chemistry II and Advanced Materials, Ulm University. In June 2011, he joined Suzhou Institute of Nano-Tech and Nano-Bionics as a professor. His research focuses on printing processing and stability of organic solar cells.

Liming Ding got his PhD from University of Science and Technology of China (was a joint student at Changchun Institute of Applied Chemistry, CAS). He started his research on OSCs and PLEDs in Olle Inganäs Lab in 1998. Later on, he worked at National Center for Polymer Research, Wright-Patterson Air Force Base and Argonne National Lab (USA). He joined Konarka as a Senior Scientist in 2008. In 2010, he joined National Center for Nanoscience and Technology as a professor. His research focuses on functional materials and devices. He is RSC Fellow, the nominator for Xplorer Prize, and the Associate Editors for Science Bulletin and Journal of Semiconductors.